Pergamon

Geochimica et Cosmochimica Acta, Vol. 68, No. 1, pp. 195–202, 2004

0016-7037/04 $30.00 + .00

doi:10.1016/S0016-7037(03)00418-6

Iodine-xenon analysis of ordinary chondrite halide: Implications for early solar system water

A. Busfield,[1,*] J. D. Gilmour,[1] J. A. Whitby,[2] and G. Turner[1]

[1]Department of Earth Sciences, University of Manchester, Manchester, M13 9PL, UK
[2]Physikalisches Institut, Universitaet Bern, Sidlerstrasse 5, 3012 Bern, Switzerland

(*Received December* 12, 2002; *accepted in revised form June* 5, 2003)

Abstract—We report the results of iodine-xenon analyses of irradiated halide grains extracted from the H-chondrite Monahans (1998) and compare them with those from Zag (Whitby et al., 2000) to address the timing of aqueous processing on the H-chondrite parent body. Xe isotopic analyses were carried out using the RELAX mass spectrometer with laser stepped heating. The initial $^{129}I/^{127}I$ ratio in the Monahans halide was determined to be $(9.37 \pm 0.06) \times 10^{-5}$ with an iodine concentration of ~400 ppb. Significant scatter, especially in the Zag data, indicates that a simple interpretation as a formation age is unreliable. Instead we propose a model whereby halide minerals in both meteorites formed ~5 Ma after the enstatite achondrite Shallowater (at an absolute age of 4559 Ma). This age is in agreement with the timing of aqueous alteration on the carbonaceous chondrite parent bodies and ordinary chondrite metamorphism and is consistent with the decay of ^{26}Al as a heat source for heating and mobilisation of brines on the H-chondrite parent body. Post accretion surface impact events may have also contributed to the heat source.

1. INTRODUCTION

Chondritic meteorites are among the most primitive solar system samples. However, they have been modified by aqueous and thermal processes during and shortly after solar system formation. The record of the aqueous processes that affected the carbonaceous chondrites has been the focus of some attention (e.g., Endress et al., 1996; Hutcheon et al., 1999). However, although the thermal history of the ordinary chondrites has been extensively studied (e.g., Dodd, 1969; Bennett and McSween, 1996; Akridge et al., 1998; Lugmair and Shukolyukov, 1998; Brazzle et al., 1999), the timing and location of their aqueous alteration and the nature of the aqueous fluids themselves are not well constrained. Here we report results of I-Xe dating of halide grains in Monahans (1998) (hereafter Monahans) and Zag that constrain the timing of aqueous processes on ordinary chondrites.

The H-chondrite Monahans fell in Monahans, Texas in 1998 (Povenmire, 1998). The meteorite is a regolith breccia consisting of light clasts and dark clasts set within a grey matrix. All three of these lithologies are H5, indicating they have experienced moderate thermal metamorphism (Zolensky et al., 1999). The shock level of the light clasts is S2, of the grey matrix is S3 and of the dark clasts is S4 (Rubin et al., 2002). Zag was observed to fall in Morocco in 1999 (Grossman, 1999). It is also an H-chondrite and contains light (H5–H6; S2–S4) and dark (H4–H5; S4–S5) clasts set in a grey clastic matrix (S2–S3) (Zolensky et al., 2000; Rubin et al., 2002).

Both Monahans and Zag contain halide crystals (Zolensky et al., 1999). These occur as aggregates of dark blue to purple crystals and are found only in the matrix (Zolensky et al., 2000; Rubin et al., 2002). Halide crystals in Monahans commonly consist of a mixture of halite and sylvite (KCl) while those present in Zag are essentially pure halite (Zolensky et al., 2000). The Monahans halide grains are up to 5 mm in size and are the coarsest examples of halides known in a meteorite. Most of the Zag halites are less coarse (a few hundred micrometers, although aggregates range up to 1 cm) and are more common than in Monahans (Rubin et al., 2002).

Halides from both meteorites contain fluid inclusions, though they occur much more frequently in Zag than in Monahans halides (Rubin et al., 2002). The population is dominated by secondary inclusions trapped along healed fractures (~80% in Monahans) although some primary inclusions (trapped during crystal growth) are also observed (Zolensky et al., 1999). Approximately 25% of the Monahans inclusions contain vapour bubbles which are observed to move freely, indicating that the inclusions consist of a low viscosity liquid and vapour. Zolensky et al. (1999) determined this to be an aqueous salt solution suggesting that these halites formed at temperatures $<$ 100°C, perhaps much less (Zolensky et al., 1999, 2000; Rubin et al., 2002). The presence of secondary fluid inclusions is clear evidence that aqueous fluids were locally present at some time after initial halide deposition. Zolensky et al. (1999) identify two possible origins for brines such as those responsible for the formation or modification of the halides: (1) indigenous fluids flowing within the parent asteroid and (2) exogenous fluids delivered to the asteroid surface from a salt-containing icy object.

Cosmogenic nuclides in the silicate matrices of Monahans and Zag indicate a substantial residence time on or very near to the surface of the parent body. Light silicate clasts and halide material were not exposed at the surface during this time (Whitby et al., 2000; Bogard et al., 2001). Wieler et al. (2000a) reported variable K/Rb ratios in Monahans halide and Whitby et al. (2000) observed low I/Cl in Zag halite, consistent with formation by brine evaporation. The halide material therefore probably formed in the outer portions of the H-chondrite parent body by evaporation of liquid water. The silicate and halide

* Author to whom correspondence should be addressed (a.busfield@man.ac.uk).

material was probably brought together by later impact events, and then the parent Monahans and Zag materia remained buried until recent (4–6 Ma) ejection from the parent body.

Monahans halide has a model Rb-Sr age of 4.7 ± 0.2 Ga (Zolensky et al., 1999), while Bogard et al. (2001) measured a minimum Ar-Ar formation age of 4.33 ± 0.01 Ga. We have previously reported I-Xe and Ar-Ar data from fragments of Zag halite (Whitby et al., 2000) that yielded a disturbed I-Xe system and distinct ^{40}Ar-^{39}Ar plateau ages of 4.03 ± 0.05 and 4.66 ± 0.08 Ga. It was suggested that the different Ar-Ar ages may reflect the presence of an easily mobilised potassium-bearing phase.

Here we report the results of I-Xe analysis of Monahans halide and discuss both these data and those from our previous I-Xe analyses of Zag halites (Whitby et al., 2000).

2. EXPERIMENTAL

The halide grains used in this work were those previously studied by Wieler et al. (2000a) and Wieler et al. (2000b). Three grains of Monahans halide were loaded into a quartz capillary tube, which was evacuated and irradiated at the Sacavém reactor in Portugal (irradiation MN16, fast fluence of 2.6×10^{18} n cm^{-2}, thermal fluence of 1.1×10^{19} n cm^{-2}). The irradiation converts ~1 part in 10^4 of ^{127}I to ^{128}Xe, allowing a subsequent noble gas isotopic measurement to determine ^{129}I/^{127}I on closure to xenon loss. Also included in the irradiation were four chips of our irradiation monitor, the non-magnetic separate of the enstatite achondrite Shallowater (Keil et al., 1989). This is intended to allow spatial variations in fluence to be monitored and to provide a ^{127}I-^{128}Xe conversion calibration. The Shallowater samples indicated that there was no detectable spatial variation in the neutron fluence. The total mass of the halide material was 29 μg. However, when the returned irradiated material was examined only two of the grains were visible and the smaller of these disintegrated during unloading. Measurements were therefore only carried out on the largest of the grains, whose mass was estimated to be 25 ± 5 μg.

The halide sample (MH1), along with the 4 Shallowater chips (SH1–SH4) were loaded into the sample port of the Refrigerator-Enhanced Laser Analyser for Xe (RELAX) mass spectrometer (Gilmour et al., 1995) and baked overnight. Previous analysis of a halite grain from the Zag meteorite (Whitby et al., 2000) suggested that halite may degas relatively easily so a lower than normal bake temperature of ~80°C was used. Gas was released by laser stepped heating as described in Gilmour et al. (1995). Heating steps lasted for 2 min, the evolved gas was then gettered for an additional minute before being admitted to the mass spectrometer. Analysis proceeded for 5 min and the data were subsequently blank corrected and reduced as described in Gilmour et al. (1998) and Gilmour et al. (2000). Blanks were typically 2×10^{-16} cm^3 of ^{132}Xe.

The efficiency of the conversion of ^{127}I to ^{128}Xe was determined by measurements made on the Shallowater standard, assuming initial ^{129}I/^{127}I = 1.125×10^{-4} (Hohenberg, 1967). Xe analysis yielded a ^{128}Xe*/^{129}Xe* in Shallowater of 0.730 ± 0.002, corresponding to a ^{127}I to ^{128}Xe conversion efficiency of 8.2×10^{-5}. Excesses of I-derived ^{128}Xe* and the other neutron-induced isotopes were calculated over a trapped component which was assumed to be ordinary chondrite xenon (Lavielle and Marti, 1992). A uranium concentration of 6.5 ± 1.3 ppb was calculated from observed excesses of ^{134}Xe on the assumption that they were produced by neutron-induced fission of ^{235}U. No excess ^{131}Xe from neutron capture (on ^{130}Ba or ^{130}Te) was detected, indicating Ba or Te concentrations below the detection limit (<47 ppb and <6 ppb respectively).

3. RESULTS AND DISCUSSION

The Monahans data are presented in Table 1 and those of Zag from Whitby et al. (2000) are given in Table 2. The Xe released from the Monahans halide during this experiment was dominated by the isotopes ^{128}Xe and ^{129}Xe (Table 1).

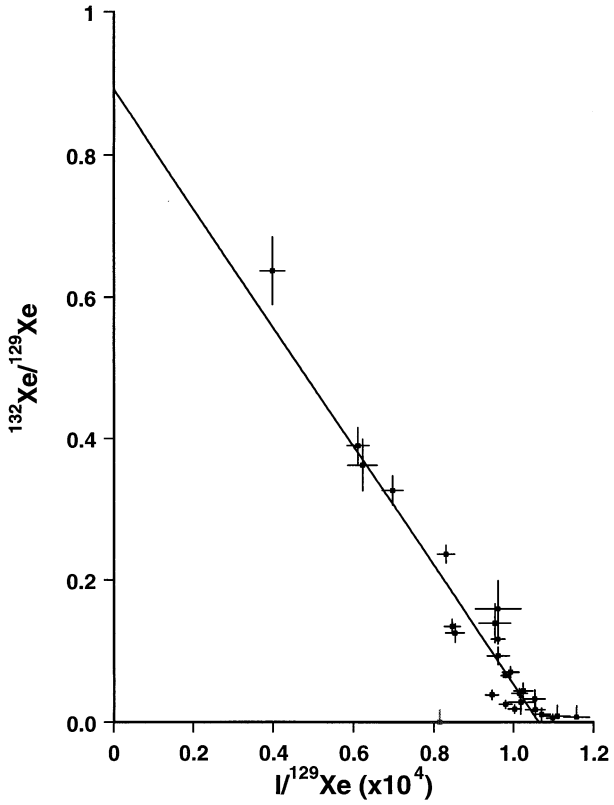

Fig. 1. A three-isotope plot of step heating data from analysis of a ~25-μg halite grain from the ordinary chondrite Monahans. Data approximate to a mixing line between a purely iodine-derived component (^{132}Xe/^{129}Xe ≡ 0) and a trapped xenon component with no associated iodine (I/^{129}Xe ≡ 0) that is consistent with ordinary chondrite xenon (Lavielle and Marti, 1992). A fit (York, 1969) to the data yields an initial iodine ratio ^{129}I/^{127}I = (9.37 ± 0.06) × 10^{-5} (corresponding to closure to xenon loss 4.15 ± 0.13 Ma after that of the Shallowater standard). The implications of significant scatter of data about the best fit line are discussed in the text.

Figure 1 shows a three-isotope plot of the Monahans data with the step release pattern displayed in Figure 2. The fit to these data yields ^{128}Xe*/^{129}Xe = 0.876 ± 0.005, corresponding to ^{129}Xe/^{127}I in the Monahans halide of (9.37 ± 0.06) × 10^{-5}. Interpreting this chronologically yields closure to xenon loss 4.15 ± 0.13 Ma after the closure of the Shallowater standard. However, Figures 1 and 2 reveal significant scatter of the data indicating that a more sophisticated interpretation may be necessary. The Zag data of Whitby et al. (2000) scatter around their mean to a much greater extent.

In Figure 3 the majority of the Monahans data are consistent with a −5 Ma isochron (closure 5 Ma after Shallowater) suggesting that this time represents a major event in the history of the halide grain. There are two probable end-member scenarios to explain the data. In the first scenario the halides formed early but a major resetting event 5 Ma after closure in Shallowater is recorded by the majority of the releases. In this case the formation age of the Monahans halide is constrained to be earlier than the oldest measured age, ~3 Ma after Shallowater (Fig. 2). The observation that the majority of the data from Monahans are consistent with −5 Ma isochron indicates

Table 1. Xe data for stepped release heating of Monahans halide (MH1). Quoted errors are 1σ.

Step	^{129}Xe × 10^{-12} cm^3 STP g^{-1}		^{129}Xe = 1															
			^{124}Xe		^{126}Xe		^{126}Xe		^{130}Xe		^{131}Xe		^{132}Xe		^{134}Xe		^{136}Xe	
MH1 sample mass = 25 ± 4 μg																		
1	368.1	2.8	0.000	0.001	0.000	0.001	1.388	0.016	0.000	0.001	0.010	0.002	0.008	0.002	0.005	0.001	0.008	0.001
2	221.1	2.2	0.000	0.001	0.000	0.001	0.877	0.009	0.000	0.003	0.000	0.003	0.000	0.003	0.001	0.002	0.000	0.002
3	124.8	1.7	0.000	0.001	0.001	0.001	0.902	0.013	0.000	0.002	0.006	0.005	0.006	0.006	0.003	0.004	0.003	0.003
4	92.5	1.5	0.000	0.002	0.001	0.002	0.825	0.014	0.001	0.002	0.015	0.006	0.018	0.006	0.006	0.004	0.007	0.004
5	86.8	1.5	0.001	0.002	0.000	0.002	0.780	0.014	0.003	0.003	0.035	0.006	0.038	0.007	0.017	0.004	0.013	0.004
6	69.2	1.5	0.001	0.003	0.000	0.003	0.821	0.018	0.001	0.003	0.059	0.007	0.070	0.008	0.035	0.005	0.029	0.005
7	39.5	1.0	0.001	0.004	0.003	0.004	0.951	0.026	0.000	0.071	0.000	0.017	0.007	0.016	0.008	0.010	0.021	0.010
8	31.2	0.9	0.002	0.005	0.007	0.005	0.839	0.027	0.000	0.010	0.036	0.016	0.028	0.018	0.007	0.011	0.010	0.010
9	51.9	1.2	0.000	0.004	0.000	0.004	0.867	0.021	0.000	0.052	0.000	0.011	0.033	0.013	0.014	0.008	0.003	0.008
10	63.5	1.4	0.000	0.003	0.001	0.003	0.845	0.020	0.000	0.050	0.010	0.010	0.044	0.012	0.020	0.007	0.013	0.007
11	46.3	1.3	0.001	0.005	0.000	0.005	0.912	0.027	0.000	0.016	0.002	0.014	0.008	0.016	0.007	0.010	0.003	0.009
12	74.7	1.7	0.000	0.003	0.002	0.003	0.944	0.021	0.000	0.020	0.000	0.020	0.000	0.022	0.000	0.007	0.000	0.006
13	124.8	2.2	0.000	0.002	0.000	0.002	0.807	0.014	0.000	0.016	0.010	0.005	0.025	0.006	0.012	0.004	0.008	0.003
14	116.7	2.3	0.000	0.003	0.000	0.003	0.837	0.016	0.000	0.003	0.031	0.006	0.040	0.007	0.020	0.004	0.013	0.004
15	42.7	0.9	0.000	0.003	0.000	0.003	0.867	0.020	0.000	0.047	0.000	0.010	0.017	0.012	0.003	0.008	0.000	0.007
16	60.5	1.3	0.000	0.003	0.002	0.003	0.936	0.020	0.000	0.012	0.000	0.013	0.000	0.013	0.000	0.008	0.000	0.005
17	63.3	1.3	0.000	0.003	0.001	0.003	0.880	0.018	0.000	0.006	0.006	0.008	0.011	0.009	0.000	0.006	0.001	0.005
18	46.0	1.1	0.000	0.004	0.001	0.004	0.857	0.022	0.000	0.013	0.000	0.012	0.000	0.014	0.000	0.009	0.006	0.008
19	41.2	1.0	0.000	0.004	0.000	0.004	0.668	0.020	0.000	0.030	0.000	0.026	0.000	0.016	0.010	0.010	0.000	0.009
20	22.8	0.9	0.000	0.008	0.001	0.008	0.794	0.033	0.026	0.010	0.112	0.024	0.139	0.028	0.058	0.017	0.046	0.016
21	25.9	0.8	0.003	0.007	0.001	0.007	0.599	0.022	0.038	0.008	0.264	0.018	0.326	0.021	0.133	0.013	0.114	0.012
22	56.5	1.3	0.001	0.004	0.001	0.004	0.706	0.017	0.017	0.004	0.112	0.009	0.134	0.011	0.059	0.007	0.050	0.006
23	37.8	1.0	0.000	0.005	0.000	0.005	0.711	0.020	0.014	0.005	0.108	0.012	0.125	0.013	0.069	0.009	0.057	0.008
24	30.6	1.1	0.001	0.009	0.000	0.009	0.948	0.035	0.009	0.009	0.000	−0.020	0.000	0.025	0.009	0.014	0.000	0.013
25	14.2	0.8	0.000	0.015	0.004	0.015	0.802	0.048	0.016	0.016	0.111	0.035	0.159	0.040	0.074	0.025	0.068	0.023
26	60.1	1.8	0.002	0.005	0.006	0.005	0.797	0.023	0.007	0.005	0.076	0.011	0.093	0.013	0.050	0.008	0.043	0.008
27	127.6	1.4	0.000	0.001	0.000	0.001	0.810	0.009	0.003	0.001	0.052	0.003	0.065	0.003	0.026	0.002	0.024	0.002
28	7.5	0.4	0.005	0.012	0.015	0.012	0.541	0.031	0.043	0.014	0.314	0.033	0.362	0.037	0.165	0.022	0.136	0.021
29	59.8	1.0	0.000	0.002	0.000	0.002	0.799	0.014	0.013	0.003	0.096	0.006	0.116	0.007	0.050	0.004	0.045	0.004
30	6.6	0.3	0.000	0.013	0.000	0.013	0.381	0.027	0.088	0.016	0.506	0.041	0.637	0.048	0.289	0.028	0.248	0.026
31	31.8	0.7	0.000	0.004	0.004	0.004	0.701	0.018	0.025	0.005	0.194	0.011	0.236	0.013	0.106	0.008	0.085	0.007
32	13.6	0.5	0.003	0.008	0.001	0.008	0.534	0.023	0.055	0.010	0.317	0.023	0.390	0.026	0.163	0.016	0.148	0.015
33	13.1	0.9	0.000	0.028	0.000	0.028	0.916	0.083	0.002	0.031	0.000	0.106	0.000	0.202	0.000	0.086	0.000	0.072
34	7.6	0.2	0.011	0.023	0.007	0.023	2.928	0.124	0.084	0.011	0.529	0.032	0.672	0.038	0.259	0.020	0.245	0.019
Total	2280.0	7.9	0.000	0.001	0.001	0.001	0.929	0.006	0.004	0.003	0.035	0.002	0.044	0.002	0.020	0.001	0.017	0.001

Tab|e 2. Xe data for stepped release heating of Zag halites (h1 and h4). A minor error in the data table of Whitby et al. (2000) has been corrected here.

Step	^{129}Xe × 10^{-12} cm^3 STP g^{-1}		^{129}Xe = 1															
			^{124}Xe		^{126}Xe		^{128}Xe		^{130}Xe		^{131}Xe		^{132}Xe		^{134}Xe		^{136}Xe	
Zag h1 sample mass = 9 μg																		
1	237.2	5.4	0.000	0.007	0.003	0.007	1.253	0.036	0.015	0.007	0.093	0.012	0.097	0.013	0.054	0.009	0.043	0.008
2	397.1	6.8	0.000	0.004	0.001	0.004	0.655	0.017	0.002	0.004	0.017	0.006	0.032	0.006	0.017	0.004	0.013	0.004
3	162.0	5.0	0.001	0.011	0.001	0.011	0.458	0.024	0.019	0.011	0.036	0.014	0.047	0.015	0.032	0.011	0.014	0.011
4	94.5	3.8	0.007	0.018	0.002	0.018	0.705	0.042	0.040	0.018	0.155	0.024	0.185	0.026	0.087	0.018	0.069	0.018
5	55.5	3.7	0.001	0.037	0.003	0.037	0.477	0.052	0.067	0.037	0.173	0.047	0.204	0.053	0.123	0.039	0.094	0.038
Total	946.2	11.3	0.001	0.004	0.002	0.004	0.766	0.019	0.016	0.004	0.062	0.006	0.076	0.007	0.042	0.005	0.031	0.004
Zag h4 sample mass = 40 μg																		
1	14.2	0.6	0.001	0.015	0.001	0.015	7.790	0.342	0.010	0.015	0.162	0.031	0.196	0.035	0.076	0.022	0.058	0.020
2	114.0	1.2	0.000	0.002	0.000	0.002	0.575	0.010	0.000	0.002	0.011	0.003	0.016	0.004	0.009	0.002	0.006	0.002
3	70.3	1.0	0.001	0.003	0.000	0.003	0.631	0.014	0.007	0.003	0.033	0.005	0.037	0.006	0.011	0.004	0.011	0.003
4	12.2	0.5	0.008	0.017	0.007	0.017	0.374	0.027	0.065	0.017	0.196	0.025	0.266	0.030	0.100	0.019	0.091	0.018
5	8.5	0.5	0.014	0.028	0.015	0.028	0.281	0.033	0.151	0.029	0.626	0.057	0.698	0.063	0.299	0.037	0.255	0.034
6	8.0	0.7	0.013	0.042	0.009	0.042	0.440	0.059	0.051	0.042	0.280	0.069	0.405	0.082	0.194	0.052	0.134	0.047
Total	227.1	1.9	0.002	0.003	0.001	0.003	1.016	0.032	0.013	0.003	0.070	0.005	0.086	0.006	0.036	0.003	0.029	0.003

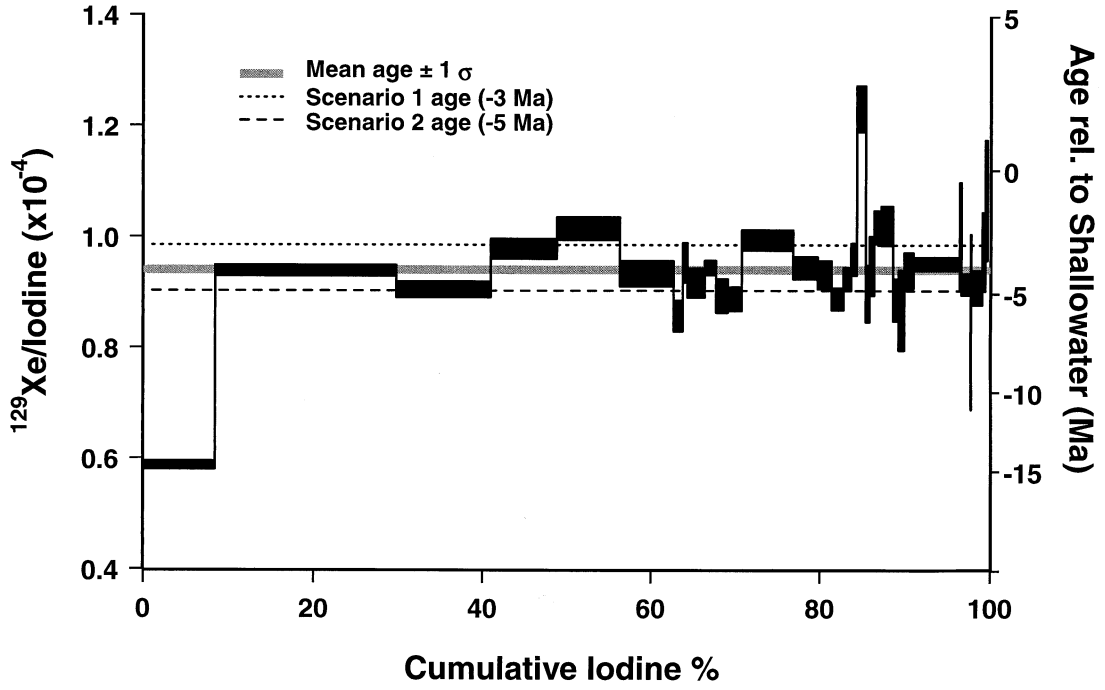

Fig. 2. Step release pattern (age spectrum) for Monahans halide. The mean age extracted from the isochron of Figure 1 is shown, as are the ages corresponding to both scenarios proposed to account for the scatter: scenario 1 (resetting) and scenario 2 (inheritance of ^{129}Xe*). Negative numbers on the right hand vertical axis indicate ages after Shallowater.

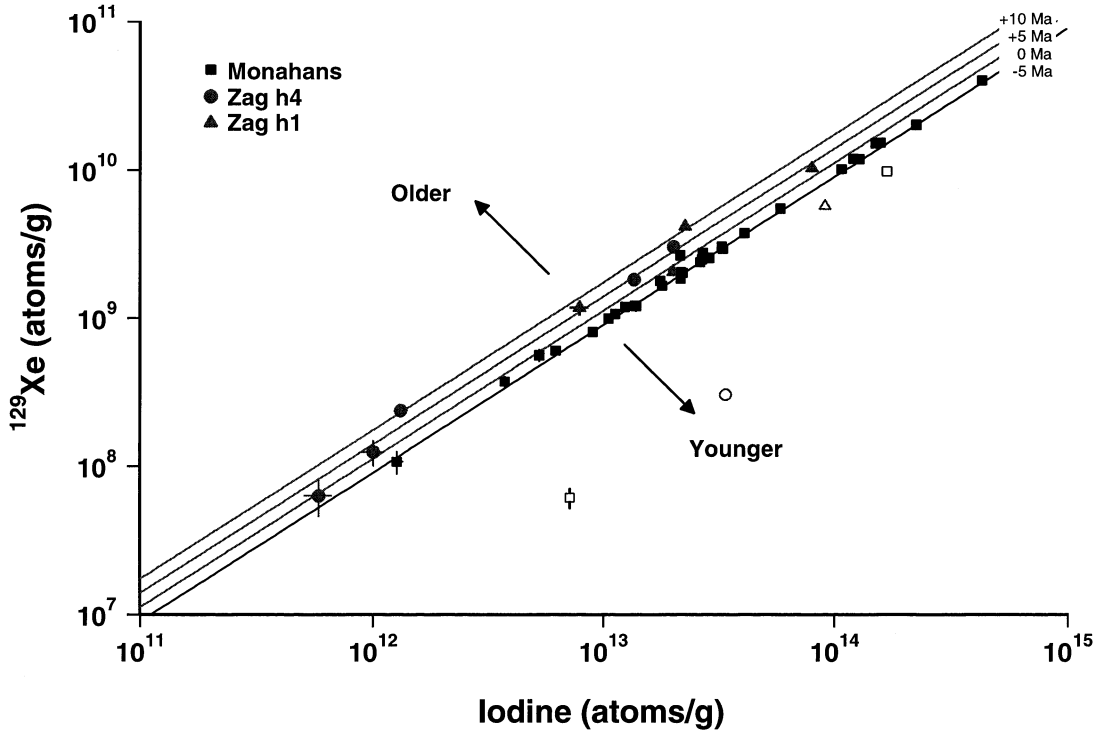

Fig. 3. Variation of ^{129}Xe concentration with iodine. Age contours relative to Shallowater are shown. The majority of the Monahans data are consistent with a −5 Ma isochron, scatter away from this tends to be towards older ages and to occur at lower iodine concentrations. Open points indicate the extreme low and high temperature releases.

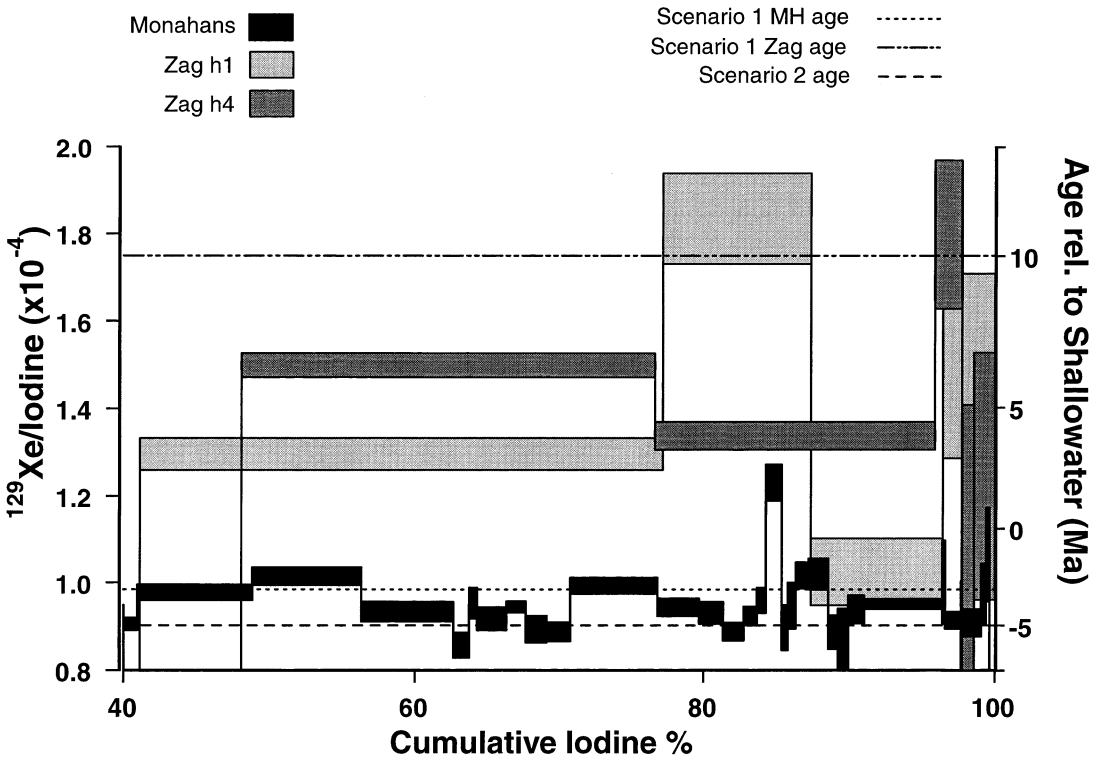

Fig. 4. High temperature step release patterns for both Zag analyses (Whitby et al., 2000). The mean age and ages corresponding to scenario 1 and scenario 2 are shown, while the pattern for Monahans halide (Fig. 2) is included for comparison.

that the disturbance event almost completely reset the I-Xe system. Extending this scenario to Zag halites would imply formation ~10 Ma before Shallowater and disturbance at about the same time as Monahans (Fig. 4). The greater degree of scatter observed in the Zag data is, under this scenario, indicative of a lesser extent of resetting than Monahans. An extreme variant of this scenario is to attribute the early ages to minor inclusions of other (i.e. not halide, perhaps silicate) material trapped within the halide grains. However, these inclusions would have to be very tiny otherwise they would have been detected by BSE imaging of the crystals (Rubin et al., 2002).

In the second scenario the −5 Ma isochron represents the formation age of the halides and an inherited component containing excess ^{129}Xe*, previously separated from its associated ^{127}I, causes the data to scatter away from the formation age towards older ages. At high iodine concentrations the parentless ^{129}Xe* would be masked by in-situ iodine-derived ^{129}Xe*. The increased scatter exhibited by the Zag data can then be understood as a consequence of its order of magnitude lower bulk iodine concentration. The calculated iodine concentration of Monahans halide is 421 ± 84 ppb (the large error on this is due to the uncertainty in estimating the mass of the halide grain), which is significantly higher than the two halite crystals from Zag (8 and 36 ppb; Whitby et al., 2000).

In Figure 5 we locate the derived formation ages of the Zag and Monahans halides in each scenario within a modified version of the chronology put forward by Gilmour and Saxton (2001). In this figure the I-Xe system is located relative to the Mn-Cr system (and so to the absolute Pb-Pb timescale) through analyses of Ste. Marguerite feldspar (for further discussion see the figure caption). Scenario 2 leads to formation of both samples at a nominal absolute age of ~4559 Ma, comparable with aqueous processing on the carbonaceous chondrite parent body. Monahans halide in scenario 1 would also yield an unremarkable age (~4561 Ma), however in this scenario Zag halite formation would be among the earliest dated events in the solar system (~4574 Ma), significantly older than the Pb-Pb age of CAIs (Amelin et al., 2002) that are usually taken to represent the earliest events in solar system history. Since halide formation must have been a parent body process, this age would require the existence of sizeable parent bodies before CAI formation. Furthermore, in Figure 3 there is a tendency for the scatter in the Monahans data to occur at lower iodine concentrations and for that scatter to predominantly tend towards earlier ages, whereas scatter would be expected to be independent of iodine concentration in scenario 1. These considerations suggest that scenario 2 (scatter to anomalously early ages due to the presence of inherited ^{129}Xe*) should be favoured.

Inherited 'parentless' ^{40}Ar, analogous to that proposed here for ^{129}Xe, is a well known phenomenon in K-Ar and Ar-Ar analyses of terrestrial samples and has been shown to be frequently associated with fluid inclusions (Kelley et al., 1986). Fluid inclusions have been reported in both Zag and Monahans halide samples, and are thus candidates for the host phase of parentless ^{129}Xe*. This would explain the greater scatter observed in Zag data—Zag halite has a greater abundance of fluid inclusions than the halide crystals from Monahans. In the Ar-Ar

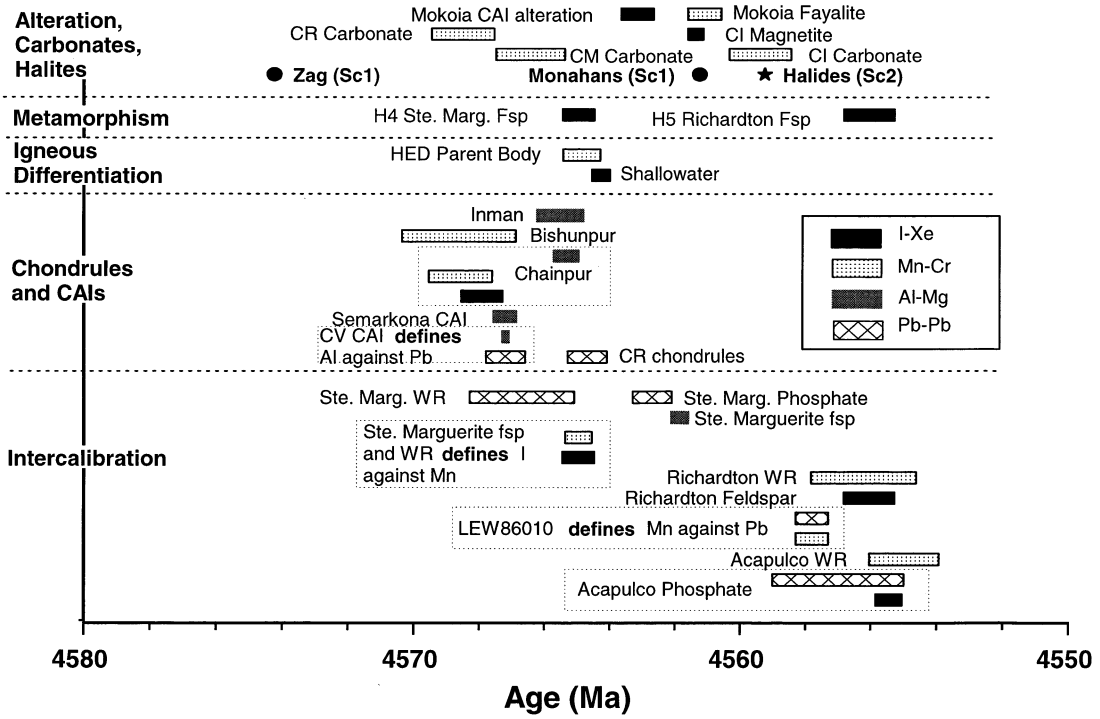

Fig. 5. A compilation of the ages obtained for various meteoritic components using a number of different isotopic dating systems (I-Xe, Mn-Cr, Al-Mg, Pb-Pb). The Mn-Cr system is anchored to the absolute Pb-Pb timescale using the angrite LEW86010, and hence an absolute age is determined for the I-Xe system by tying it to the Mn-Cr system using Ste. Marguerite feldspar and whole rock (Gilmour and Saxton, 2001). Absolute ages for Al-Mg are inferred by anchoring it to the Pb-Pb system in CAIs (Amelin et al., 2002). Apparent I-Xe ages derived for the Zag and Monahans halides corresponding to scenarios 1 and 2 are shown. Zag halite has an anomalously early formation age in scenario 1 that, combined with other evidence, leads us to favour scenario 2. Acapulco phosphate: Brazzle et al. (1999) and Göpel et al. (1992); Acapulco whole rock: Lugmair and Shukolyukov (1998); LEW86010: Lugmair and Shukolyukov (1998) and Lugmair and Galer (1992); Richardton feldspar: Brazzle et al. (1999); Richardton whole rock: Polnau and Lugmair (2001); Ste. Marguerite whole rock: Polnau and Lugmair (2001) and Göpel et al. (1994); Ste. Marguerite feldspar: Brazzle et al. (1999) and Zinner and Göpel (2002); Ste. Marguerite phosphate: Göpel et al. (1994); CV CAI: Amelin et al. (2002); CR chondrules: Amelin et al. (2002); Semarkona CAI: Russell et al. (1996); Chainpur: Russell et al. (1996), Nyquist et al. (2001) and Swindle et al. (1991); Bishunpur: Nyquist et al. (2001); Inman: Russell et al. (1996); Shallowater: Brazzle et al. (1999); HED parent body: Lugmair and Shukolyukov (1998); CM carbonate: Hutcheon et al. (1999); CI carbonate: Endress et al. (1996); CR carbonate: Hutcheon et al. (1999); CI magnetite: Hohenberg et al. (2000); Mokoia fayalite: Hutcheon et al. (1998).

system, the presence of inherited $^{40}Ar^*$ can be inferred due to a correlation with ^{38}Ar produced from chlorine during neutron irradiation, chlorine being used as a proxy for the fluid (typically brines). Such a clear cut identification is impossible in the I-Xe system since the halogen from which we could infer the presence of a brine (iodine) is also the parent of ^{129}Xe. In principle the $^{129}Xe^*/^{38}Ar^*$ ratio could be used to search for brines bearing parentless $^{129}Xe^*$ but not in a Cl-bearing mineral such as halite. The higher iodine concentration in Monahans halide may be due to the presence of sylvite, which is absent in Zag (Rubin et al., 2002). There is some evidence from seawater evaporation curves that concentrations of iodine in sylvite are higher than in halite precipitated from the same brine (Zherebtsova and Volkova, 1966; Holser, 1979).

The creation of a 'parentless' component requires chemical separation of parent from daughter after a period of decay. This might occur, for instance, when the parent preferentially partitions into a crystallising phase or when the daughter element is removed from the host mineral of the parent (perhaps by leaching, in which case a fluid enriched in the decay product would be produced). Partition coefficients for iodine substitution into salt crystals are extremely low (Holser, 1979), thus little or no fractionation of Xe from I is expected to have occurred as halite and sylvite crystallised in Zag and Monahans. This suggests that we must look to a separate mechanism for the generation of any parentless $^{129}Xe^*$. From these partition coefficients we would also expect that any of the primary fluid would be enriched in iodine. Therefore, the primary fluid inclusions are perhaps an unlikely source of $^{129}Xe^*$. The secondary inclusions identified by Zolensky et al. (1999) are a more plausible candidate for the host phase since they would have had a distinct history of interactions with iodine-bearing phases from which the parentless $^{129}Xe^*$ could be derived. Some combination of the two is also possible. However, since neither halide sample represents the product of a closed system formation, model ages obtained by dividing total excess ^{129}Xe by total iodine may have little or no significance.

The identification of an inherited component with parentless

^{129}Xe* has the potential to seriously complicate the interpretation of the iodine-xenon system. However, the situation is mitigated somewhat by the rarity of fluid inclusions in meteorite samples. The potential for misinterpretation as an age only exists where iodine and a component with parentless ^{129}Xe* are trapped together in a consistent ratio, and where trapped planetary xenon that can act as a tracer of fluid is not also present. Excesses of ^{129}Xe without iodine have been identified previously, and we have recently shown (Gilmour et al., 2001) how a mixed iodine-xenon component may be responsible for the appearance of an evolving iodine-xenon system in some analyses of suites of chondrules. Thus the effects of inherited 'parentless' ^{129}Xe* may be more apparent in derived trapped compositions than in anomalous ages.

4. THE EVOLUTION OF THE H-CHONDRITE PARENT BODY

In Figure 5 we have presented a compilation of apparent absolute ages of chondrules, CAIs and meteoritic components, produced by a variety of aqueous and thermal parent body processes, using a number of different isotopic dating systems. Here we adopt the halide age of scenario 2 and consider implications for models of parent body evolution.

In principle, the water responsible for aqueous effects on chondritic parent bodies could have originated either from within the parent body or could have been delivered to the surface by icy impactors. Whilst external bodies almost certainly contributed water on a local scale the presence of ubiquitous aqueous effects in many chondrites suggests a widespread internal source. Rubin et al. (2002) consider dehydration of phyllosilicates incorporated into parent bodies during accretion as the most plausible origin for this water. However, melting of nebular ice accreted with the parent body may also have contributed.

Ice melting or dehydration reactions and subsequent mobilisation of water require a heat source. There are a number of possibilities: surface impacts (which may also deliver water ice), decay of long-lived nuclides or decay of short-lived nuclides. The comparatively late age of scenario 2 precludes impacts associated with accretion as the heat source. Post accretion, individual impact heating events will have been of short duration but may have occurred at late ages, so this source is a clear possibility. The ages of halide and other aqueous products are consistent with chondritic metamorphism and achondritic differentiation ages so ^{26}Al decay ($t_{1/2}$ = 0.73 Ma) may be seen as a plausible heat source for generation and mobilisation of the liquid water responsible for halide deposition on the H-chondrite parent body (e.g., Nichols et al., 1994; Lugmair and Shukolyukov, 1998). Detailed modelling of water transport through a carbonaceous chondrite parent body, initially heated by ^{26}Al decay, suggests that liquid water could have persisted for millions of years (Cohen and Coker, 2000). The model of fluid flow on carbonaceous chondrite planetesimals proposed by Young et al. (1999) is not directly applicable to the H-chondrite parent body due to probable differences in size, composition and physical properties. In this model Young et al. (1999) suggest that fluid would have ceased to flow after < 1 Ma on their 25-km radius body which, in the light of ages determined for aqueous alteration products (Fig. 5), seems unrealistic unless some of these parent bodies formed very late. Modelling of the temperature evolution of ordinary chondrite parent bodies also indicates that conditions sufficient for the presence of liquid water existed for many millions of years (Akridge et al., 1998). However, all these models indicate the presence of a frozen outer shell which never attains adequate temperatures for the existence and evaporation of liquid water. Depending on the depth of formation of the halides analysed in this study local impact heating may have played an important role.

Terrestrial evaporites typically contain fluid inclusions and sylvite intergrowths, and the presence of such features in the halides studied here suggests that these also formed by brine evaporation. Evaporation and halide precipitation took place fairly slowly in a low temperature environment (<100°C, probably 25–50°C; Rubin et al., 2002) which thermal models predict would have been found at depths of a few kilometres (Akridge et al., 1998). This contrasts with the higher metamorphic temperatures inferred for H5 chondritic material such as that surrounding the halide in Monahans. Bogard et al. (2001) found that Monahans silicate material was irradiated on the surface of its parent body. However, regions very near the surface would have been too cold to support liquid water (Akridge et al., 1998; Wilson et al., 1999) indicating a depth of a few kilometers for halide formation, additionally (Whitby et al., 2000) suggested on the basis of the spallation history that Zag halite was not present when the regolith was exposed at the surface. This suggests that the halides must have been introduced to the surface after their formation, presumably by impacts. Late assembly of halite and regolith is also necessary because the I-Xe age of resetting of feldspar in the H5 chondrite Richardton is later than that of (low-temperature) halite formation (Fig. 5). Thus the two components must have been separate during this epoch and subsequently assembled as a result of impact processing of the parent body.

In summary, we are in a position to advance a simple description of the origin of halides in samples of the H-chondrite parent body. The halides formed within a few km of the surface as evaporites. The heat source may have been associated with that of metamorphism of the parent body, though an external water source is also a possibility. Iodine was incorporated into the halite preserved in Zag as it formed, while samples of the parent fluid were trapped in inclusions. A subsequent generation of secondary fluid inclusions were trapped along fractures—this fluid may contain 'parentless' ^{129}Xe*. Sufficient ^{129}Xe* is associated with the fluid inclusions to affect the I-Xe systematics of the bulk sample. In Monahans, sylvite formation led to a much higher iodine concentration in the solid phase, allowing it to more effectively dominate the I-Xe system and record the formation age more faithfully. At some point after the interior of the H chondrite parent body had cooled, impacts brought H5 material to the surface where it was irradiated by cosmic rays. Further gardening mixed the halite and the irradiated H5 silicates to produce the assemblage observed in the meteorites today. This later event may be recorded by the 4-Ga Ar-Ar age of one Zag sample.

Acknowledgments—We are very grateful to M. Zolensky and R. Wieler for originally separating the halide material and for permission to use it in this study. We thank D. J. Blagburn and B. Clementson for

technical support. This work was supported by PPARC and the Royal Society through a University Research Fellowship (JDG). Helpful reviews were provided by D. Bogard, A. Rubin and M. Zolensky. Additional comments by R. Wieler were invaluable.

Associate editor: R. Wieler.

REFERENCES

Akridge G., Benoit P. H., and Sears D. W. G. (1998) Regolith and megaregolith formation of H-chondrites: Thermal constraints on the parent body. *Icarus* **132,** 185–195.

Amelin Y., Krot A. N., Hutcheon I. D., and Ulyanov A. A. (2002) Lead isotopic ages of chondrules and calcium-aluminium-rich inclusions. *Science* **297,** 1678–1683.

Bennett I. M. E. and McSween J. H. Y. (1996) Revised model calculations for the thermal histories of ordinary chondrite parent bodies. *Meteorit. Planet. Sci.* **31,** 783–792.

Bogard D. D., Garrison D. H., and Masarik J. (2001) The Monahans chondrite and halite: Argon-39/argon-40 age, solar gases, cosmic-ray exposure ages, and parent body regolith neutron flux thickness. *Meteorit. Planet. Sci.* **36,** 107–122.

Brazzle R. H., Pravdivtseva O. V., Meshik A. P., and Hohenberg C. M. (1999) Verification and interpretation of the I-Xe chronometer. *Geochim. Cosmochim. Acta* **63,** 739–760.

Cohen B. A. and Coker R. F. (2000) Modelling of liquid water on CM meteorite parent bodies and implications for amino acid racemization. *Icarus* **145,** 369–381.

Dodd R. T. (1969) Metamorphism of the ordinary chondrites: A review. *Geochim. Cosmochim. Acta* **33,** 161–203.

Endress M., Zinner E., and Bischoff A. (1996) Early aqueous activity on primitive meteorite parent bodies. *Nature* **379,** 701–703.

Gilmour J. D. and Saxton J. M. (2001) A time-scale of formation of the first solids. *Philos. Trans. R. Soc. London, Ser. A* **359,** 2037–2048.

Gilmour J. D., Ash R. D., Bridges J. C., Lyon I. C., and Turner G. (1995) Iodine-xenon studies of Bjurböle and Parnallee using RELAX. *Meteoritics* **30,** 405–411.

Gilmour J. D., Whitby J. A., and Turner G. (1998) Xenon isotopes in irradiated ALH84001: Evidence for shock-induced trapping of ancient Martian atmosphere. *Geochim. Cosmochim. Acta* **62,** 2555–2571.

Gilmour J. D., Whitby J. A., Turner G., Bridges J. C., and Hutchison R. (2000) The iodine-xenon system in clasts and chondrules from ordinary chondrites: Implications for early solar system chronology. *Meteorit. Planet. Sci.* **35,** 445–455.

Gilmour J. D., Whitby J. A., and Turner G. (2001) Negative correlation of iodine-129/iodine-127 and xenon-129/xenon-132: Product of closed-system evolution or evidence of a mixed component. *Meteorit. Planet. Sci.* **36,** 1283–1286.

Göpel C., Manhès G., and Allègre C. J. (1992) U-Pb systematics of phosphates from equilibrated ordinary chondrites. *Earth Planet. Sci. Lett.* **121,** 153–171.

Göpel C., Manhès G., and Allègre C. J. (1994) U-Pb study of the Acapulco meteorite. *Meteoritics* **27,** 226.

Grossman J. N. (1999) The Meteoritical Bulletin. *Meteorit. Planet. Sci.* **34 (***Suppl.***),** A169.

Hohenberg C. M. (1967) I-Xe dating of the Shallowater achondrite. *Earth Planet. Sci. Lett.* **3,** 357–362.

Hohenberg C. M., Pravdivtseva O., and Meshik A. (2000) Reexamination of anomalous I-Xe ages: Orgueil and Murchison magnetites and Allegan feldspar. *Geochim. Cosmochim. Acta* **64,** 4257–4262.

Holser W. T. (1979) Trace elements and isotopes in evaporites. In *Marine Minerals*, Vol. 6 (ed. R. G. Burns), pp. 298–346. Mineral Society of America.

Hutcheon I. D., Krot A. N., Keil K., Phinney D. L., and Scott E. R. D. (1998) ^{53}Mn-^{53}Cr dating of fayalite formation in the CV3 chondrite Mokoia: Evidence for asteroidal alteration. *Science* **282,** 1865–1867.

Hutcheon I. D., Browning L., Keil K., Krot A. N., Phinney D. L., Prinz M., and Weisberg M. K. (1999) Time scale of aqueous activity in the early solar system. *Ninth Ann. V. M. Goldschmidt Conf.*, abstract #7491 [CD-ROM]. LPI contribution no. 971, Lunar and Planetary Institute, Houston, TX.

Keil K., Ntaflos T., Taylor G. J., Brearley A. J., Newsom H. E., and Romig A. D., Jr. (1989) The Shallowater aubrite: Evidence for origin by planetesimal impacts. *Geochim. Cosmochim. Acta* **53,** 3291–3307.

Kelley S., Turner G., Butterfield A. W., and Shepherd T. J. (1986) The source and significance of argon isotopes in fluid inclusions from areas of mineralization. *Earth Planet. Sci. Lett.* **79,** 303–318.

Lavielle B. and Marti K. (1992) Trapped xenon in ordinary chondrites. *J. Geophys. Res.* **97,** 20875–20881.

Lugmair G. W. and Galer S. J. G. (1992) Age and isotopic relationships among the angrites Lewis Cliff-86010 and Angra-dos-Reis. *Geochim. Cosmochim. Acta* **56,** 1673–1694.

Lugmair G. W. and Shukolyukov A. (1998) Early solar system timescales according to ^{53}Mn-^{53}Cr systematics. *Geochim. Cosmochim. Acta* **62,** 2863–2886.

Nichols R. H., Jr., Hohenberg C. M., Kehm K., Kim Y., and Marti K. (1994) I-Xe studies of the Acapulco meteorite: Absolute I-Xe ages of individual phosphate grains and the Bjurböle standard. *Geochim. Cosmochim. Acta* **58,** 2553–2561.

Nyquist L., Lindstrom D., Mittlefehldt D., Shih C-Y., Wiesmann H., Wentworth S., and Martinez R. (2001) Manganese-chromium formation intervals for chondrules from the Bishunpur and Chainpur meteorites. *Meteorit. Planet. Sci.* **36,** 911–938.

Polnau E., and Lugmair G. W (2001) Mn-Cr isotope systematics in the two ordinary chondrites Richardton (H5) and Ste. Marguerite (H4). *Lunar Planet. Sci. Conf.* **32,** abstract #1527 [CD-ROM].

Povenmire H. (1998) The Monahans, Texas, meteorite fall of March 22, 1998. *Meteorit. Planet. Sci.* **33,** A125–A126.

Rubin A. E., Zolensky M. E., and Bodnar R. J. (2002) The halite-bearing Zag and Monahans (1998) meteorite breccias: Shock metemorphism, thermal metamorphism and aqueous alteration on the H-chondrite parent body. *Meteorit. Planet. Sci.* **37,** 125–141.

Russell S. S., Srinivasan G., Huss G. R., Wasserburg G. J., and MacPherson G. J. (1996) Evidence for widespread ^{26}Al in the solar nebula and constraints for nebula time scales. *Science* **273,** 757–762.

Swindle T. D., Caffee M. W., Hohenberg C. M., Lindstrom M. M., and Taylor G. J. (1991) Iodine-xenon studies of petrographically and chemically characterized Chainpur chondrules. *Geochim. Cosmochim. Acta* **55,** 861–880.

Whitby J., Burgess R., Turner G., Gilmour J., and Bridges J. (2000) Extinct ^{129}I in halite from a primitive meteorite: Evidence for evaporite formation in the early solar system. *Science* **288,** 1819–1821.

Wieler R., Günther D., Hattendorf B., Leya I., Pettke T., Vogel N., and Zolensky M. E. (2000a) The chemical composition and light noble gas data of halite in the Monahans regolithic breccia. *Meteorit. Planet. Sci.* **35** (Suppl.)**,** A170–A170.

Wieler R., Günther D., Hattendorf B., Pettke T., and Zolensky M. E. (2000b) Chemical composition of halite from the Monahans chondrite determined by laser ablation ICP-MS. *Lunar Planet. Sci. Conf.* **31,** abstract #1560 [CD-ROM].

Wilson L., Keil K., Browning L. B., Krot A. N., and Bourcier W. (1999) Early aqueous alteration, explosive disruption, and reprocessing of asteroids. *Meteorit. Planet. Sci.* **34,** 541–557.

York D. (1969) Least squares fitting of a straight line with correlated errors. *Earth Planet. Sci. Lett.* **5,** 320–324.

Young E. D., Ash R. D., England P., and Rumble D. III. (1999) Fluid flow in chondritic parent bodies: Deciphering the compositions of planetesimals. *Science* **286,** 1331–1335.

Zherebtsova L. K, Volkova N. N (1966) Experimental study of behavior of trace elements in the process of natural solar evaporation of Black Sea water and Sasyk-Sivash brine. *Geokhimiya* 832–845.

Zinner E. and Göpel C. (2002) Aluminium-26 in H4 chondrites: Implications for its production and its usefulness as a fine-scale chronometer for early solar system events. *Meteorit. Planet. Sci.* **37,** 1001–1013.

Zolensky M. E., Bodnar R. J., Gibson E. K., Jr., Nyquist L. E., Reese Y., Shih C.-Y., and Wiesmann H. (1999) Asteroidal water within fluid inclusion–bearing halite in an H5 chondrite, Monahans (1998). *Science* **285,** 1377–1379.

Zolensky M. E., Bodnar R. J., Schwandt C., and Yang S. V. (2000) Halide minerals in the Monahans (1998) and Zag H chondrite regolith breccias. *Lunar Planet. Sci. Conf.* **31,** abstract #1181 [CD-ROM].